Genetic and transgenic reagents for *Drosophila simulans*, *D. mauritiana*, *D. yakuba*, *D. santomea* and *D. virilis*

David L. Stern[1*], Justin Crocker[1], Yun Ding[1], Nicolas Frankel[2], Gretchen Kappes[3], Elizabeth Kim[1], Ryan Kuzmickas[4], Andrew Lemire[1] and Serge Picard[5]

[1] *Janelia Research Campus, 19700 Helix Drive, Ashburn, Virginia 20147, USA*

[2] *Departamento de Ecologıa, Genetica y Evolucion, IEGEBA-CONICET, Facultad de Ciencias Exactas y Naturales, Universidad de Buenos Aires, Ciudad Universitaria, Pabellon 2, C1428EHA Buenos Aires, Argentina*

[3] *Current address unknown*

[4] *Genetics Division, Department of Medicine, Brigham and Women's Hospital, Boston, Massachusetts 02115, USA*

[5] *Lewis-Sigler Institute for Integrative Genomics, Carl Icahn Laboratory, Washington Road, Princeton University, Princeton, NJ 08544*

*Address correspondence and requests for reagents to sternd@janelia.hhmi.org

Abstract

Species of the *Drosophila melanogaster* species subgroup, including the species *D. simulans*, *D. mauritiana*, *D. yakuba*, and *D. santomea*, have long served as model systems for studying evolution. Studies in these species have been limited, however, by a paucity of genetic and transgenic reagents. Here we describe a collection of transgenic and genetic strains generated to facilitate genetic studies within and between these species. We have generated many strains of each species containing mapped *piggyBac* transposons including an *enhanced yellow fluorescent protein* gene expressed in the eyes and a phiC31 *attP* site-specific integration site. We have tested a subset of these lines for integration efficiency and reporter gene expression levels. We have also generated a smaller collection of other lines expressing other genetically encoded fluorescent molecules in the eyes and a number of other transgenic reagents that will be useful for functional studies in these species. In addition, we have mapped the insertion locations of 86 transposable elements in *D. virilis* that will be useful for genetic mapping studies.

Keywords: *Drosophila*, genetics, transgenics, phi-C31 integrase, speciation, evolution

Ever since Alfred Sturtevant discovered *Drosophila simulans*, the sister species to *D. melanogaster*, in 1919, species of the *Drosophila melanogaster* species subgroup have played a central role in studies of evolution and speciation (Powell 1997; Barbash 2010). Most species of the subgroup display superficially similar anatomy, although all species can be distinguished by both qualitative and quantitative anatomical differences (Orgogozo and Stern 2009). In addition, the species display enormous variation in ecology and behavior, with some having evolved into ecological specialists on unusual food sources (R'Kha *et al.* 1991; Yassin *et al.* 2016).

One of the major advantages of this subgroup for evolutionary studies is that many of the species can be crossed to *D. melanogaster* to generate sterile hybrids and some can be crossed to each other to generate fertile hybrid females (Powell 1997). An unusual and important feature of these fertile pairs is that strains of each species can be found that share synteny across entire chromosomes (Lemeunier and Ashburner 1976; Moehring *et al.* 2006a). This allows comprehensive genetic interrogation of entire chromosomes through recombination mapping. This is an uncommon feature for fertile pairs of *Drosophila* species; most species that have been examined exhibit major chromosomal inversions that are fixed between species (Powell 1997).

We were motivated by the phenotypic variability and genetic accessibility of these species to establish a set of reagents that would allow, simultaneously, a platform for site-specific transgenesis (Groth *et al.* 2004) and reagents useful for genetic mapping studies.

The combination of relatively straightforward genetics with diversity in anatomy, physiology and behavior has encouraged many groups to perform genetic analyses of these species (e.g. Liu *et al.* 1996; True *et al.* 1997; Macdonald and Goldstein 1999; Gleason and Ritchie 2004; Moehring *et al.* 2004, 2006a; b; Carbone *et al.* 2005; Gleason *et al.* 2005; Orgogozo *et al.* 2006; Cande *et al.* 2012; Arif *et al.* 2013; Peluffo *et al.* 2015). In the vast majority of cases, however, these studies have stopped after quantitative trait locus (QTL) mapping of traits of interest. One factor that has limited further genetic study of these traits is a limited set of genetic markers, which can facilitate fine-scale mapping. John True and Cathy Laurie established a large collection of strains

carrying *P-element* transposons marked with a w^+ mini-gene in a *w*- background of *D. mauritiana* (True *et al.* 1996a; b). These have been used for introgression studies (True *et al.* 1996b; Coyne and Charlesworth 1997; Tao *et al.* 2003a; b; Masly and Presgraves 2007; Masly *et al.* 2011; Arif *et al.* 2013; Tanaka *et al.* 2015; Tang and Presgraves 2015) and for high-resolution mapping studies (McGregor *et al.* 2007; Araripe *et al.* 2010), demonstrating the utility of dominant genetic markers for evolutionary studies. One limitation of these strains is that the w^+ marker is known to induce behavioral artifacts (Zhang and Odenwald 1995; Campbell and Nash 2001; Xiao and Robertson 2016). We have also observed that mutations in the *white* gene and some w^+ rescue constructs cause males to generate abnormal courtship song (unpublished data). Other pigmentation genes that are commonly used in *D. melanogaster* are also known to disrupt normal behavior (Bastock 1956; Kyriacou *et al.* 1978; Drapeau *et al.* 2006; Suh and Jackson 2007). It would be preferable, therefore, to employ dominant genetic markers that do not interfere with normal eye color or pigmentation.

We therefore set out to establish a collection of strains carrying transposable elements marked with innocuous dominant markers for four of the most commonly studied species of the *D. melanogaster* species subgroup: *D. simulans*, *D. mauritiana*, *D. yakuba* and *D. santomea*. We chose the *piggyBac* transposable element to minimize bias of insertion sites relative to gene start sites (Thibault *et al.* 2004) and integrated transposable elements carrying *enhanced yellow fluorescent protein* (*EYFP*) and *DsRed* driven by a *3XP3* enhancer that usually drives expression in the eyes (Horn *et al.* 2003). A large subset of the lines described here also include a phiC31 *attP* landing site to facilitate site-specific transgene integration to common landing sites within each species. Here we describe the establishment and mapping of many lines of each species carrying *pBac*{*3XP3*::*EYFP,attP*} and *pBac*{*3XP3*::*DsRed*} (Horn *et al.* 2003). We have characterized a subset of the *pBac*{*3XP3*::*EYFP,attP*} lines from each species for phiC31 integration efficiency of plasmids containing an *attB* sequence. In addition, we have integrated transgenes driving expression in the *even-skipped* stripe 2 domain to characterize embryonic expression generated by a subset of *attP* landing sites. We have employed CRISPR/Cas9 to knock out the *3XP3::EYFP* genes in a subset of lines to facilitate integration of reagents for neurogenetics. We also describe several other genetic and transgenic reagents that may be useful to the community, including the map positions for *pBac* transposons integrated in the *D. virilis* genome.

Methods

Transposable elements employed: We used *piggyBac* transposable elements (Horn *et al.* 2003) to mobilize markers to random locations within the genomes of *D. simulans white*[501] (San Diego Species Stock Center stock number 14021-0251.011), *D. simulans yellow*[1] *white*[1] (San Diego Species Stock Center stock number 14021-0251.013), *D. mauritiana white*$^-$ (San Diego Species Stock Center stock number 14021-0241.60), *D. yakuba white*$^-$ (San Diego Species Stock Center stock number 14021-0261.02), *D. santomea* STO CAGO 1482 (provided by Peter Andolfatto), and *D. virilis w*[50112] (San Diego Species Stock Center number 15010-1051.53). We constructed *pBac*{*3XP3*::*EYFP-attP*} by cloning a BglII fragment containing the *attP* site from *pM*{*3XP3-RFPattP'*} (Bischof *et al.* 2007) into the single BglII site of *pBac*{*3XP3*::*EYFPafm*} (Horn and Wimmer 2000).

We constructed *pBac* plasmids carrying a source of *P*-element transposase marked with *3XP3*::*EYFP* or *3XP3*::*DsRed* as follows. We digested the plasmid pACNNTNPII-S129A (Beall *et al.* 2002) with EcoRI and NotI and cloned the ~5kb fragment resulting from digestion into pSLFa1180fa (Horn and Wimmer 2000). This plasmid was digested with AscI or FseI and the ~5kb fragment was cloned into the AscI or FseI restriction sites of *pBac*{*3XP3*::*DsRed*} or *pBac*{*3XP3*::*EGFP,attP*} (Horn and Wimmer 2000) to generate *pBac*{*Pactin*::*Ptrsps, 3XP3*::*DsRed*} and *pBac*{ *Pactin*::*Ptrsps 3XP3*::*EGFP,attP*}, respectively. These plasmids were injected into strains of *D. simulans* and *D. mauritiana*.

We also injected *pBac*{*3XP3*::*DsRed*} (Horn *et al.* 2003) into strains of *D. simulans*, *D. mauritiana*, *D. yakuba*, and *D. santomea*.

The complete sequences of *pBac*{*3XP3*::*EYFP-attP*}, *pBac*{*3XP3*::*DsRed*} and *phsp-pBac* are provided as Supplementary Material.

These plasmids were co-injected with 250 ng/uL *phsp-pBac* (Handler and Harrell 1999), a heat-shock inducible source of *piggyBac* transposase, and one hour after injection embryos were heat shocked at 37°C for one hour. All embryo injections were performed by Rainbow Transgenic Flies Inc. G0 flies were backcrossed to un-injected flies of the same strain and G1 flies were screened for fluorescence in their eyes.

Fluorescence could be detected easily in all of the *white*$^-$ strains (*D. simulans, D. mauritiana, D. yakuba*, and *D. virilis*) using any dissecting microscope we tried with epi-fluoresence capability. However, we found that fluorescence could not be detected in eyes of flies with wild type eye coloration using a Leica 165 FC stereomicroscope. This microscope uses "TripleBeam Technology" to deliver excitation light along a separate light path from the emission light. Unfortunately, the excitation light in this system appears to illuminate ommatidia adjacent to the ommatidia that are viewed for the emission light. Therefore, fluorescence cannot be detected in these flies. We therefore recommend avoiding the Leica microscopes with "TripleBeam Technology" when screening for eye fluorescence in flies with wild-type eye color.

Mapping of transposable element insertion sites: We mapped the genomic insertion sites of all *pBac* elements using both inverse PCR (Ochman *et al.* 1988) and TagMap (Stern 2016). Inverse PCR (iPCR) was not ideal for our project for

several reasons. First, many isolated strains appeared to contain multiple insertion events, even though they were isolated from single G0 animals. These multiple events could sometimes be detected by segregation of offspring with multiple strengths of fluorescence in the eyes. In these cases, sometimes iPCR produced uninterpretable sequences and sometimes apparently only a single insertion event amplified. Second, many iPCR sequences were too short to allow unambiguous mapping to the genome. Third, sometimes iPCR reactions failed for no obvious reason. For all of these reasons, it was difficult to unambiguously map all of the *pBac* insertions with iPCR. We therefore developed and applied TagMap (Stern 2016) to map the insertion positions of all *pBac* elements. Tagmap provided map positions for all but a few strains.

Mapping *pBac* transposon insertion sites in *D. virilis*: We previously generated multiple *pBac* insertions into *D. virilis* to study the *svb* gene (Frankel *et al.* 2012). However, none of these *pBac* insertions have been mapped previously. These reagents may be useful for genetic mapping studies. We have therefore mapped positions of these inserts using TagMap.

Generation of a *D. santomea white-* allele: We began to generate this collection of reagents prior to the availability of a *white*$^-$ strain of *D. santomea.* However, soon after CRISPR/Cas9-mediated genome editing became available, we generated a *white*$^-$ strain derived from *D. santomea* STO-CAGO 1482 as follows. *In vitro* transcribed Cas9 mRNA, generated with an EcoRI digested T7-*Cas9* template plasmid and the mMESSAGE mMACHINE T7 Transcription Kit (ThermoFisher Scientific), together with two gRNAs targeting the third exon of the *white* gene were injected into pre-blastoderm embryos by Rainbow Transgenics. The sequence for the T7-*Cas9* plasmid is provided as Supplementary Data. The gRNAs were generated by separate *in vitro* transcription reactions, using the MEGAscript T7 Transcription Kit (ThermoFisher Scientific), of PCR amplified products of the following forward and reverse primers: Forward primer CRISPRF-san-w12, 5' GAA ATT AAT ACG ACT CAC TAT AGG CAA CCT GTA GAC GCC AGT TTT AGA GCT AGA AAT AGC; Forward primer CRISPRF-san-w17, 5' GAA ATT AAT ACG ACT CAC TAT AGG GCC ACG CGC TGC CGA TGT TTT AGA GCT AGA AAT AGC; Reverse primer gRNA-scaffold, 5' AAA AGC ACC GAC TCG GTG CCA CTT TTT CAA GTT GAT AAC GGA CTA GCC TTA TTT TAA CTT GCT ATT TCT AGC TCT AAA AC. All PCR reactions described in this paper were performed using Phusion High Fidelity DNA Polymerase (NEB) using standard conditions. Injected G0 flies were brother-sister mated and G1 flies were screened for white eyes. Once we identified a *white*$^-$ strain, we backcrossed the *pBac*{*3XP3*::*EYFP-attP*} markers generated previously in *D. santomea* STO-CAGO 1482 to the *white*$^-$ strain. The *pBac* insertion sites in these new *white*$^-$ strains were then re-mapped with TagMap.

Testing phiC31-mediated integration efficiency: Different *attP* landing sites provide different efficiencies of integration of *attB*-containing plasmids (Bischof *et al.* 2007). We performed a preliminary screen of integration efficiency on a subset of the *attP* landing sites we generated. Pre-blastoderm embryos were co-injected with 250 ng/uL of plasmids containing *attB* sites and 250 ng/uL pBS130 (Gohl *et al.* 2011), a heat-shock inducible source of phiC31 integrase, and one hour after injection were incubated at 37°C for one hour. G0 offspring were backcrossed to the parental line and G1 offspring were screened for the relevant integration marker. We performed this screen using a heterogeneous collection of plasmids that we are integrating for other purposes. Therefore, the integration efficiencies we report are not strictly comparable between sites. Nonetheless, we were able to identify a subset of sites that provide reasonable integration efficiency and which can be made homozygous after integration of transgenes. We report these statistics for all sites that we have tested (Supplementary File: Strains and Integration Efficiencies.xlsx).

Testing expression patterns and levels of transgenes integrated in different *attP* sites: Different *attP* landing sites drive different levels and patterns of transgene expression (Pfeiffer *et al.* 2010). We have tested a subset of the *attP* sites in our collection for embryonic expression of an integrated *D. melanogaster even-skipped* stripe 2 enhancer (Small *et al.* 1992). Plasmid *D. melanogaster eveS2-placZ* was co-injected with 250 ng/uL pBS130 into approximately ten *pBac*{*3XP3::EYFP-attP*} strains of each species and we isolated transgenic lines for seven *D. simulans*, four *D. mauritiana*, two *D. yakuba* strains, and four *D. santomea* strains. We performed fluorescent in situ hybridization and imaged mid-stage 5 embryos on a Leica TCS SPE confocal microscope. Embryos of all samples were scanned with equal laser power to allow quantitative comparisons of expression patterns between strains.

We performed staining experiments for all sites from each species in parallel; embryo collection, fixation, hybridization, image acquisition, and processing were performed side-by-side under identical conditions. Confocal exposures were identical for each series. Image series were acquired in a single day, to minimize signal loss. Sum projections of confocal stacks were assembled, embryos were scaled to match sizes, background was subtracted using a 50-pixel rolling-ball radius and fluorescence intensity was analyzed using ImageJ software (http://rsb.info.nih.gov/ij/).

Killing *EYFP* expression from *attP* landing sites: Expression of the *EYFP* genes associated with the *attP* sites may conflict with some potential uses of the *attP* landing sites, for example for integration of transgenes driving *GFP*-derivatives, such as *GCaMP*, in the brain. We have therefore started generating *pBac*{*3XP3*::*EYFP-attP*} strains where we have killed the *EYFP* activity using CRISPR-Cas9 mediated targeted mutagenesis. We first built a derivative of the *pCFD4-U61-U63* tandem gRNAs plasmid (Port *et al.* 2014) where we replaced the *vermillion* marker with a *3XP3*::*DsRed* dominant marker. The *vermillion* marker was removed by HindIII digestion of pCFD4-U61-U63 and isolation of the 5,253 bp band. The *3XP3*::*DsRed* cassette was amplified from a *pUC57*{*3xP3*::*DsRed*} plasmid using the following primers:

5' TAC GAC TCA CTA TAG GGC GAA TTG GGT ACA CCA GTG AAT TCG AGC TCG GT, 5' TTG GAT GCA GCC TCG AGA TCG ATG ATA TCA ATT ACG CCA AGC TTG CAT GC. The PCR product and vector backbone were assembled with Gibson assembly (Gibson *et al.* 2009) following http://openwetware.org/wiki/Gibson_Assembly to generate *p{CFD4-3xP3::DsRed-BbsI}*. To remove the BbsI restriction site from *DsRed*, which conflicts with the BbsI restriction site used for cloning gRNA sequences, we digested this plasmid with NcoI and isolated the ~6kb fragment, PCR amplified this region with primers that eliminated the BbsI restriction site (Forward primer: 5' CGG GCC CGG GAT CCA CCG GTC GCC ACC ATG GTG CGC TCC TCC AAG AAC GTC A, Reverse primer: 5' CGC TCG GTG GAG GCC TCC CAG CCC ATG GTT TTC TTC TGC ATT ACG GGG CC), and Gibson cloned the PCR product into the plasmid backbone. This yielded plasmid *p{CFD4-3xP3::DsRed}*.

To make a plasmid for mutating *EYFP* in fly lines, we digested *p{CFD4-3xP3::DsRed}* with BbsI and gel purified the 5,913 bp fragment. A gBlocks Gene Fragment (IDT) (5' CAA GTA CAT ATT CTG CAA GAG TAC AGT ATA TAT AGG AAA GAT ATC CGG GTG AAC TTC GGG TGG TGC AGA TGA ACT TCA GTT TTA GAG CTA GAA ATA GCA AGT TAA AAT AAG GCT AGT CCG TTA TCA ACT TG), which contained a gRNA sequence targeting EYFP that was previously validated by direct injection was synthesized and Gibson assembled with the BbsI digested fragment of *p{CFD4-3xP3::DsRed}* to make *p{CFD4-EYFP-3xP3::DsRed}*.

This plasmid contains *attB* and can be integrated into *attP* sites. We tested this by integrating this plasmid into the *attP* site of *D. simulans* line 930. This plasmid is a potent source of gRNA targeting EYFP, which we confirmed by crossing this line to a transgenic strain carrying *nos-Cas9*. (We have previously reported our production of transgenic strains of *Drosophila simulans*, *D. mauritiana*, and *D. yakuba* carrying *nos-Cas9* on the website maintained by Philip Port: http://www.crisprflydesign.org/).

To knockout *EYFP* in specific strains carrying *pBac{3XP3::EYFP-attP}*, we co-injected 500 ng/uL *in vitro* transcribed Cas9 mRNA and 250 ng/uL *p{CFD4-EYFP-3xP3::DsRed}*. G0 individuals were brother-sister mated and we screened for reduction or loss of *EYFP* expression in G1 progeny. Individuals displaying reduced or no *EYFP* expression were crossed to generate strains homozygous for *EYFP⁻*.

Results

Generation and mapping of *pBac{3XP3::EYFP-attP}* strains: We generated many strains carrying *pBac{3XP3::EYFP-attP}* and *pBac{3XP3::DsRed}* insertions, mapped these, and culled the collection to unique lines that could be maintained as homozygotes. The final collection includes 184 *D. simulans* lines, 122 *D. mauritiana* lines, 104 *D. yakuba* lines, 64 *D. santomea* lines, and nine *D. virilis* lines. Maps indicating the insertion site locations are shown in Figures 1-5 and are provided as searchable Geneious files (http://www.geneious.com/) in Supplementary Material. Details of the transgenic strains are provided in Supplementary Data: Strains and Integration Efficiencies.xlsx.

Mapping *pBac* transposon insertion sites in *D. virilis*: To assist with genetic experiments in *D. virilis,* we mapped the insertion locations for all *pBac* lines generated in our lab for a previously published study (Frankel *et al.* 2012). These results are shown in Figure 5 and available in a Geneious file and Supplementary Data: Strains and Integration Efficiencies.xlsx.

Testing phiC31-mediated integration efficiency: We tested efficiency of integration of *attB* plasmids into *attP* landing sites of multiple strains of each species. Some landing sites in *D. simulans*, *D. mauritiana*, *D. santomea* and *D. yakuba* supported integration of *attB* plasmids, although many landing sites did not support integration at reasonable frequency. In addition, we tested nine *D. virilis* strains carrying *pBac{3XP3::EYFP-attP}* and did not recover any integrants. There are strong differences in integration efficiencies between landing sites. Details of integration efficiencies for each line are provided in Supplementary Data: Strains and Integration Efficiencies.xlsx.

Testing expression patterns of transgenes integrated in different *attP* sites: We integrated a *D. melanogaster eveS2-placZ* plasmid into multiple *attP* landing site strains of each species to examine variability in expression at different landing sites. Levels of reporter gene expression varied between strains (Figure 6). In *D. simulans*, *D. mauritiana*, and *D. yakuba*, we identified at least one strain that drove strong and temporal-spatially accurate levels of *eveS2* expression. However, of the four landing sites we tested in *D. santomea*, none provided strong expression of *eveS2* (Figure 6 & 7). *eveS2* transgenes often drive weak, spatially diffuse expression prior to stage 5, and all of the *D. santomea* strains displayed similar diffuse, weak expression at early stages. We also observed ectopic expression of the *eveS2* transgene in *D. santomea 2092* (Figure 7h). It is not clear if the poor expression of *eveS2* in these *D. santomea* landing sites reflects differential regulation of the *D. melanogaster eveS2* enhancer in *D. santomea* or suppression of expression caused by position effects of these specific landing sites.

Unmarked attP landing sites: To facilitate integration of plasmids expressing fluorescent proteins that overlap with the excitation and emission spectrum of EYFP, we have generated a subset of strains in which we induced null mutations in the *EYFP* gene marking the *attP* landing sites. These strains were generated by CRISPR/Cas9-induced mutagenesis. All strains were sequenced to ensure that the mutations did not disrupt the *attP* landing site. We have so far generated two strains in *D. mauritiana*, and three strains in each of *D. santomea*, *D. simulans* and *D. yakuba* (Supplementary Material). We continue to generate *EYFP*-knockout strains for other *attP* landing sites and we will update the stock list associated with this manuscript as new lines are generated.

Discussion

We have generated a collection of transgenic strains that will be useful for multiple kinds of experiments. First, the *3XP3*::*EYFP-attP* strains provide a collection of *attP* landing sites for each species that will facilitate transgenic assays in these species. Integration efficiencies vary widely between strains and our experiments provide some guidance toward identifying landing sites with the highest efficiency of integration. Second, these transgenes carry markers that will be useful for genetic mapping experiments. Several published studies have already used these reagents and illustrate the power of these strains for genetic studies (Andolfatto *et al.* 2011; Erezyilmaz and Stern 2013; Ding *et al.* 2016).

We have generated transgenic strains using these *attP* landing sites and found that they show variation in embryonic expression patterns (Figures 6 & 7). These results provide a rough guide to which strains may be useful for experiments that require low or high levels of embryonic expression. However, these results may not be predictive of transgene expression patterns at other developmental stages and in other tissues and we strongly encourage colleagues to test a variety of landing sites for their experiments and report their experiences to us. We plan to continue to maintain a database reporting on integration efficiencies and expression patterns and we will periodically update the Excel file associated with this manuscript.

This collection of reagents complements the existing resources available for studying species of the genus *Drosophila*, including the availability of multiple genome sequences (Clark *et al.* 2007) and BAC resources (Song *et al.* 2011). This resource will accelerate research on gene function in diverse *Drosophila* species and the study of evolution in the genus *Drosophila*.

Conflict of Interest:

The authors declare no competing financial interests.

Acknowledgements:

Most fly stocks were provided by the San Diego Species Stock Center and *D. santomea* STO CAGO 1482 was kindly provided by Peter Andolfatto. We thank Ernst Wimmer for providing the original *piggyBac* reporter plasmids. We thank Dennis Eckmeier (www.eckmeier.de) for the bioRXiv Word template.

Author Contributions:

DLS conceived of the project. NF made *pBac{3XP3*::*EYFP-attP}*. DLS, YD, and GK screened injected flies for integration events. YD, RK, AL, J-YK and SP performed iPCR experiments. JYK prepared DNA samples for TagMap. DLS performed TagMap. AL and SP sequenced the TagMap libraries. DLS, YD, GK, and JYK performed the genetics. JC performed the embryo *in situ* hybridization experiments. DLS wrote the paper.

Requests for Reagents:

All plasmids have been deposited with Addgene and all requests for plasmids should be directed to Addgene (plasmid IDs 86860 – 86864). All fly stocks are maintained in the Stern lab at Janelia Research Campus and all requests for fly stocks should be directed to David Stern. The raw iPCR and TagMap data are available upon request to David Stern.

References

Andolfatto P., Davison D., Erezyilmaz D., Hu T. T., Mast J., Sunayama-Morita T., Stern D. L., 2011 Multiplexed shotgun genotyping for rapid and efficient genetic mapping. Genome Res. **21**: 610–7.

Araripe L. O., Montenegro H., Lemos B., Hartl D. L., 2010 Fine-scale genetic mapping of a hybrid sterility factor between Drosophila simulans and D. mauritiana: the varied and elusive functions of "speciation genes". BMC Evol. Biol. **10**: 385.

Arif S., Hilbrant M., Hopfen C., Almudi I., Nunes M. D. S., Posnien N., Kuncheria L., Tanaka K., Mitteroecker P., Schlötterer C., Mcgregor A. P., 2013 Genetic and developmental analysis of differences in eye and face morphology between Drosophila simulans and Drosophila mauritiana. Evol. Dev. **15**: 257–267.

Barbash D. A., 2010 Ninety years of Drosophila melanogaster hybrids. Genetics **186**: 1–8.

Bastock M., 1956 A Gene Mutation Which Changes a Behavior Pattern. Evolution (N. Y). **10**: 421–439.

Beall E. L., Mahoney M. B., Rio D. C., 2002 Identification and analysis of a hyperactive mutant form of Drosophila P-element transposase. Genetics **162**: 217–227.

Bischof J., Maeda R. K., Hediger M., Karch F., Basler K., 2007 An optimized transgenesis system for Drosophila using germ-line-specific phiC31 integrases. Proc Natl Acad Sci U S A **104**: 3312–3317.

Campbell J. L., Nash H. A., 2001 Volatile general anesthetics reveal a neurobiological role for the white and brown genes of Drosophila melanogaster. J. Neurobiol. **49**: 339–349.

Cande J., Andolfatto P., Prud'homme B., Stern D. L., Gompel N., 2012 Evolution of multiple additive loci caused divergence between Drosophila yakuba and D. santomea in wing rowing during male courtship. PLoS One **7**: e43888.

Carbone M. A., Llopart A., deAngelis M., Coyne J. A., Mackay T. F., 2005 Quantitative trait loci affecting the difference in pigmentation between Drosophila yakuba and D. santomea. Genetics **171**: 211–225.

Clark A. G., Eisen M. B., Smith D. R., Bergman C. M., Oliver B., Markow T. A., Kaufman T. C., Kellis M., Gelbart W., Iyer V.

N., Pollard D. A, Sackton T. B., Larracuente A. M., Singh N. D., Abad J. P., Abt D. N., Adryan B., Aguade M., Akashi H., Anderson W. W., Aquadro C. F., Ardell D. H., Arguello R., Artieri C. G., Barbash D. a, Barker D., Barsanti P., Batterham P., Batzoglou S., Begun D., Bhutkar A., Blanco E., Bosak S. A., Bradley R. K., Brand A. D., Brent M. R., Brooks A. N., Brown R. H., Butlin R. K., Caggese C., Calvi B. R., Bernardo de Carvalho A., Caspi A., Castrezana S., Celniker S. E., Chang J. L., Chapple C., Chatterji S., Chinwalla A., Civetta A., Clifton S. W., Comeron J. M., Costello J. C., Coyne J. a, Daub J., David R. G., Delcher A. L., Delehaunty K., Do C. B., Ebling H., Edwards K., Eickbush T., Evans J. D., Filipski A., Findeiss S., Freyhult E., Fulton L., Fulton R., Garcia A. C. L., Gardiner A., Garfield D. a, Garvin B. E., Gibson G., Gilbert D., Gnerre S., Godfrey J., Good R., Gotea V., Gravely B., Greenberg A. J., Griffiths-Jones S., Gross S., Guigo R., Gustafson E. a, Haerty W., Hahn M. W., Halligan D. L., Halpern A. L., Halter G. M., Han M. V, Heger A., Hillier L., Hinrichs A. S., Holmes I., Hoskins R. a, Hubisz M. J., Hultmark D., Huntley M. a, Jaffe D. B., Jagadeeshan S., Jeck W. R., Johnson J., Jones C. D., Jordan W. C., Karpen G. H., Kataoka E., Keightley P. D., Kheradpour P., Kirkness E. F., Koerich L. B., Kristiansen K., Kudrna D., Kulathinal R. J., Kumar S., Kwok R., Lander E., Langley C. H., Lapoint R., Lazzaro B. P., Lee S.-J. J., Levesque L., Li R., Lin C.-F. F., Lin M. F., Lindblad-Toh K., Llopart A., Long M., Low L., Lozovsky E., Lu J., Luo M., Machado C. a, Makalowski W., Marzo M., Matsuda M., Matzkin L., McAllister B., McBride C. S., McKernan B., McKernan K., Mendez-Lago M., Minx P., Mollenhauer M. U., Montooth K., Mount S. M., Mu X., Myers E., Negre B., Newfeld S., Nielsen R., Noor M. a F., O'Grady P., Pachter L., Papaceit M., Parisi M. J. M. J., Parts L., Pedersen J. S., Pesole G., Phillippy A. M., Ponting C. P., Pop M., Porcelli D., Powell J. R., Prohaska S., Pruitt K., Puig M., Quesneville H., Ram K. R., Rand D., Rasmussen M. D., Reed L. K., Reenan R., Reily A., Remington K. a, Rieger T. T., Ritchie M. G., Robin C., Rogers Y.-H. H., Rohde C., Rozas J., Rubenfield M. J., Ruiz A., Russo S., Salzberg S. L., Sanchez-Gracia A., Saranga D. J., Sato H., Schaeffer S. W., Schatz M. C., Schlenke T., Schwartz R., Segarra C., Singh R. S., Sirot L., Sirota M., Sisneros N. B., Smith C. D., Smith T. F., Spieth J., Stage D. E., Stark A., Stephan W., Strausberg R. L., Strempel S., Sturgill D., Sutton G. G., Tao W., Teichmann S., Tobari Y. N., Tomimura Y., Tsolas J. M., Valente V. L. S., Venter E., Venter J. C., Vicario S., Vieira F. G., Vilella A. J., Villasante A., Walenz B., Wang J., Wasserman M., Watts T., Wilson D., Wilson R. K., Wing R. a, Wolfner M. F., Wong A., Wong G. K.-S., Wu C.-I. I., Wu G., Yamamoto D., Yang H.-P. P., Yang S.-P. P., Yorke J. A., Yoshida K., Zdobnov E., Zhang P., Zhang Y., Zimin A. V, Baldwin J., Abdouelleil A., Abdulkadir J., Abebe A., Abera B., Abreu J., Acer S. C., Aftuck L., Alexander A., An P., Anderson E., Anderson S., Arachi H., Azer M., Bachantsang P., Barry A., Bayul T., Berlin A., Bessette D., Bloom T., Blye J., Boguslavskiy L., Bonnet C., Boukhgalter B., Bourzgui I., Brown A., Cahill P., Channer S., Cheshatsang Y., Chuda L., Citroen M., Collymore A., Cooke P., Costello M., D'Aco K., Daza R., Haan G. De, DeGray S., DeMaso C., Dhargay N., Dooley K., Dooley E., Doricent M., Dorje P., Dorjee K., Dupes A., Elong R., Falk J., Farina A., Faro S., Ferguson D., Fisher S., Foley C. D., Franke A., Friedrich D., Gadbois L., Gearin G., Gearin C. R., Giannoukos G., Goode T., Graham J., Grandbois E., Grewal S., Gyaltsen K., Hafez N., Hagos B., Hall J., Henson C., Hollinger A., Honan T., Huard M. D., Hughes L., Hurhula B., Husby M. E., Kamat A., Kanga B., Kashin S., Khazanovich D., Kisner P., Lance K., Lara M., Lee W., Lennon N., Letendre F., LeVine R., Lipovsky A., Liu X., Liu J., Liu S., Lokyitsang T., Lokyitsang Y., Lubonja R., Lui A., MacDonald P., Magnisalis V., Maru K., Matthews C., McCusker W., McDonough S., Mehta T., Meldrim J., Meneus L., Mihai O., Mihalev A., Mihova T., Mittelman R., Mlenga V., Montmayeur A., Mulrain L., Navidi A., Naylor J., Negash T., Nguyen T., Nguyen N., Nicol R., Norbu C., Norbu N., Novod N., O'Neill B., Osman S., Markiewicz E., Oyono O. L., Patti C., Phunkhang P., Pierre F., Priest M., Raghuraman S., Rege F., Reyes R., Rise C., Rogov P., Ross K., Ryan E., Settipalli S., Shea T., Sherpa N., Shi L., Shih D., Sparrow T., Spaulding J., Stalker J., Stange-Thomann N., Stavropoulos S., Stone C., Strader C., Tesfaye S., Thomson T., Thoulutsang Y., Thoulutsang D., Topham K., Topping I., Tsamla T., Vassiliev H., Vo A., Wangchuk T., Wangdi T., Weiand M., Wilkinson J., Wilson A., Yadav S., Young G., Yu Q., Zembek L., Zhong D., Zimmer A., Zwirko Z., Alvarez P., Brockman W., Butler J., Chin C., Grabherr M., Kleber M., Mauceli E., MacCallum I., 2007 Evolution of genes and genomes on the Drosophila phylogeny. Nature **450**: 203–18.

Coyne J. A., Charlesworth B., 1997 Genetics of a Pheromonal Difference Affecting Sexual Isolation Between Drosophila mauritianu and D. sechellia. Genetics **145**: 1015–1030.

Ding Y., Berrocal A., Morita T., Longden K. D., Stern D. L., 2016 Natural courtship song variation caused by an intronic retroelement in an ion channel gene. Nature **536**: 329–332.

Drapeau M. D., Cyran S. A., Viering M. M., Geyer P. K., Long A. D., 2006 A cis-regulatory sequence within the yellow locus of Drosophila melanogaster required for normal male mating success. Genetics **172**: 1009–1030.

Erezyilmaz D. F., Stern D. L., 2013 Pupariation Site Preference Within and Between Drosophila Sibling Species. Evolution (N. Y). **67**: 2714–2727.

Frankel N., Wang S., Stern D. L., 2012 Conserved regulatory architecture underlies parallel genetic changes and convergent phenotypic evolution. Proc. Natl. Acad. Sci. U. S. A. **109**: 20975–9.

Gibson D. G., Young L., Chuang R.-Y., Venter J. C., Iii C. A. H., Smith H. O., America N., Hutchison C. a, 2009 Enzymatic assembly of DNA molecules up to several hundred kilobases. Nat. Methods **6**: 343–5.

Gleason J. M., Ritchie M. G., 2004 Do quantitative trait loci (QTL) for a courtship song difference between Drosophila simulans and D. sechellia coincide with candidate genes and intraspecific QTL? Genetics **166**: 1303–1311.

Gleason J. M., Jallon J. M., Rouault J. D., Ritchie M. G., 2005 Quantitative trait loci for cuticular hydrocarbons associated with sexual isolation between Drosophila simulans and D. sechellia. Genetics **171**: 1789–1798.

Gohl D. M., Silies M. A., Gao X. J., Bhalerao S., J. F. L., Lin C.-C.,

Potter C. J., Clandinin T. R., 2011 A versatile in vivo system for directed dissection of gene expression patterns. Nat Methods **8**: 231–237.

Groth A. C., Fish M., Nusse R., Calos M. P., 2004 Construction of Transgenic Drosophila by Using the Site-Specific Integrase From Phage {phi}C31. Genetics **166**: 1775–1782.

Handler A. M., Harrell R. A. 2nd, 1999 Germline transformation of Drosophila melanogaster with the piggyBac transposon vector. Insect Mol. Biol. **8**: 449–457.

Horn C., Wimmer E. a, 2000 A versatile vector set for animal transgenesis. Dev. Genes Evol. **210**: 630–7.

Horn C., Offen N., Nystedt S., Hacker U., Wimmer E. A., 2003 piggyBac-Based Insertional Mutagenesis and Enhancer Detection as a Tool for Functional Insect Genomics. Genetics **163**: 647–661.

Kyriacou C. P. P., Burnet B., Connolly K., 1978 The behavioural basis of overdominance in competitive mating success at the ebony locus of Drosophila melanogaster. Anim. Behav. **26**: 1195–1206.

Lemeunier F., Ashburner M. a, 1976 Relationships within the melanogaster species subgroup of the genus Drosophila (Sophophora). II. Phylogenetic relationships between six species based upon polytene chromosome banding sequences. Proc. R. Soc. Lond. B. Biol. Sci. **193**: 275–94.

Liu J., Nercer J. M., Stam L. F., Gibson G. C., Zeng Z.-B. B., Laurie C. C., Mercer J. M., Stam L. F., Gibson G. C., Zeng Z.-B. B., Laurie C. C., 1996 Genetic analysis of a morphological shape difference in the male genitalia of Drosophila simulans and D-mauritiana. Genetics **142**: 1129–1145.

Macdonald S. J., Goldstein D. B., 1999 A quantitative genetic analysis of male sexual traits distinguishing the sibling species Drosophila simulans and D. sechellia. Genetics **153**: 1683–1699.

Masly J. P., Presgraves D. C., 2007 High-resolution genome-wide dissection of the two rules of speciation in Drosophila. PLoS Biol **5**: e243.

Masly J. P., Dalton J. E., Srivastava S., Chen L., Arbeitman M. N., 2011 The genetic basis of rapidly evolving male genital morphology in Drosophila. Genetics **189**: 357–374.

McGregor A. P., Orgogozo V., Delon I., Zanet J., Srinivasan D. G., Payre F., Stern D. L., 2007 Morphological evolution through multiple cis-regulatory mutations at a single gene. Nature **448**: 587–590.

Moehring A. J., Li J., Schug M. D., Smith S. G., deAngelis M., Mackay T. F., Coyne J. A., 2004 Quantitative trait loci for sexual isolation between Drosophila simulans and D. mauritiana. Genetics **167**: 1265–1274.

Moehring A. J., Llopart A., Elwyn S., Coyne J. A., Mackay T. F., 2006a The genetic basis of prezygotic reproductive isolation between Drosophila santomea and D. yakuba due to mating preference. Genetics **173**: 215–223.

Moehring A. J., Llopart A., Elwyn S., Coyne J. A., Mackay T. F., 2006b The genetic basis of postzygotic reproductive isolation between Drosophila santomea and D. yakuba due to hybrid male sterility. Genetics **173**: 225–233.

Ochman H., Gerber A. S., Hartl D. L., 1988 Genetic applications of an inverse polymerase chain reaction. Genetics **120**: 621–623.

Orgogozo V., Broman K. W., Stern D. L., 2006 High-resolution quantitative trait locus mapping reveals sign epistasis controlling ovariole number between two Drosophila species. Genetics **173**: 197–205.

Orgogozo V., Stern D. L., 2009 How different are recently diverged species ? Fly (Austin). **3**: 117.

Peluffo A. E., Nuez I., Debat V., Savisaar R., Stern D. L., Orgogozo V., 2015 A Major Locus Controls a Genital Shape Difference Involved in Reproductive Isolation Between Drosophila yakuba and Drosophila santomea. G3 (Bethesda).: g3.115.023481-.

Pfeiffer B. D., Ngo T. T., Hibbard K. L., Murphy C., Jenett A., Truman J. W., Rubin G. M., 2010 Refinement of tools for targeted gene expression in Drosophila. Genetics **186**: 735–755.

Port F., Chen H., Lee T., Bullock S. L., 2014 Optimized CRISPR / Cas tools for efficient germline and somatic genome engineering in Drosophila. PNAS.

Powell J. R., 1997 *Progress and prospects in evolutionary biology: The Drosophila model*. Oxford University Press, Oxford.

R'Kha S., Capy P., David J. R., 1991 Host-plant specialization in the Drosophila melanogaster species complex: a physiological, behavioral, and genetical analysis. Proc. Natl. Acad. Sci. U. S. A. **88**: 1835–9.

Small S., Blair A., Levine M., 1992 Regulation of even-skipped stripe 2 in the Drosophila embryo. EMBO J. **11**: 4047–4057.

Song X., Goicoechea J. L., Ammiraju J. S. S., Luo M., He R., Lin J., Lee S. J., Sisneros N., Watts T., Kudrna D. A., Golser W., Ashley E., Collura K., Braidotti M., Yu Y., Matzkin L. M., McAllister B. F., Markow T. A., Wing R. A., 2011 The 19 genomes of Drosophila: A BAC library resource for genus-wide and genome-scale comparative evolutionary research. Genetics **187**: 1023–1030.

Stern D. L., 2016 Tagmentation-Based Mapping (TagMap) of Mobile DNA Genomic Insertion Sites. bioRxiv: 1–7.

Suh J., Jackson F. R., 2007 Drosophila Ebony Activity Is Required in Glia for the Circadian Regulation of Locomotor Activity. Neuron **55**: 435–447.

Tanaka K. M., Hopfen C., Herbert M. R., Schlotterer C., Stern D. L., Masly J. P., McGregor a. P., Nunes M. D. S., 2015 Genetic Architecture and Functional Characterization of Genes Underlying the Rapid Diversification of Male External Genitalia Between Drosophila simulans and Drosophila mauritiana. Genetics **200**: 357–369.

Tang S., Presgraves D. C., 2015 Lineage-specific evolution of the complex Nup160 hybrid incompatibility between Drosophila melanogaster and its sister species. Genetics **200**: 1245–1254.

Tao Y., Chen S., Hartl D. L., Laurie C. C., 2003a Genetic dissection of hybrid incompatibilities between Drosophila simulans and D. mauritiana. I. Differential accumulation of hybrid male sterility effects on the X and autosomes. Genetics **164**: 1383–1397.

Tao Y., Zeng Z. B., Li J., Hartl D. L., Laurie C. C., 2003b Genetic dissection of hybrid incompatibilities between Drosophila simulans and D. mauritiana. II. Mapping hybrid male sterility loci on the third chromosome. Genetics **164**: 1399–1418.

Thibault S. T., Singer M. A., Miyazaki W. Y., Milash B., Dompe N. A., Singh C. M., Buchholz R., Demsky M., Fawcett R., Francis-Lang H. L., Ryner L., Cheung L. M., Chong A., Erickson C., Fisher W. W., Greer K., Hartouni S. R., Howie E., Jakkula L., Joo D., Killpack K., Laufer A., Mazzotta J., Smith R. D., Stevens L. M., Stuber C., Tan L. R., Ventura R., Woo A., Zakrajsek I., Zhao L., Chen F., Swimmer C., Kopczynski C., Duyk G., Winberg M. L., Margolis J., 2004 A complementary transposon tool kit for Drosophila melanogaster using P and piggyBac. Nat Genet **36**: 283–287.

True J. R., Mercer J. M., Laurie C. C., 1996a Differences in crossover frequency and distribution among three sibling species of Drosophila. Genetics **142**: 507–523.

True J. R., Weir B. S., Laurie C. C., 1996b A genome-wide survey of hybrid incompatibility factors by the introgression of marked segments of Drosophila mauritiana chromosomes into Drosophila simulans. Genetics **142**: 819–837.

True J. R., Liu J., Stam L. F., Zeng Z.-B. Z.-B., Laurie C. C., 1997 Quantitative genetic analysis of divergence in male secondary sexual traits between Drosophila simulans and Drosophila mauritiana. Evolution (N. Y). **51**: 816–832.

Xiao C., Robertson R. M., 2016 Timing of locomotor recovery from anoxia modulated by the white gene in Drosophila. Genetics **203**: 787–797.

Yassin A., Debat V., Bastide H., Gidaszewski N., David J. R., Pool J. E., 2016 Recurrent specialization on a toxic fruit in an island Drosophila population. Proc. Natl. Acad. Sci. U. S. A.: 201522559.

Zhang S. D., Odenwald W. F., 1995 Misexpression of the white (w) gene triggers male-male courtship in Drosophila. Proc. Natl. Acad. Sci. **92**: 5525–5529.

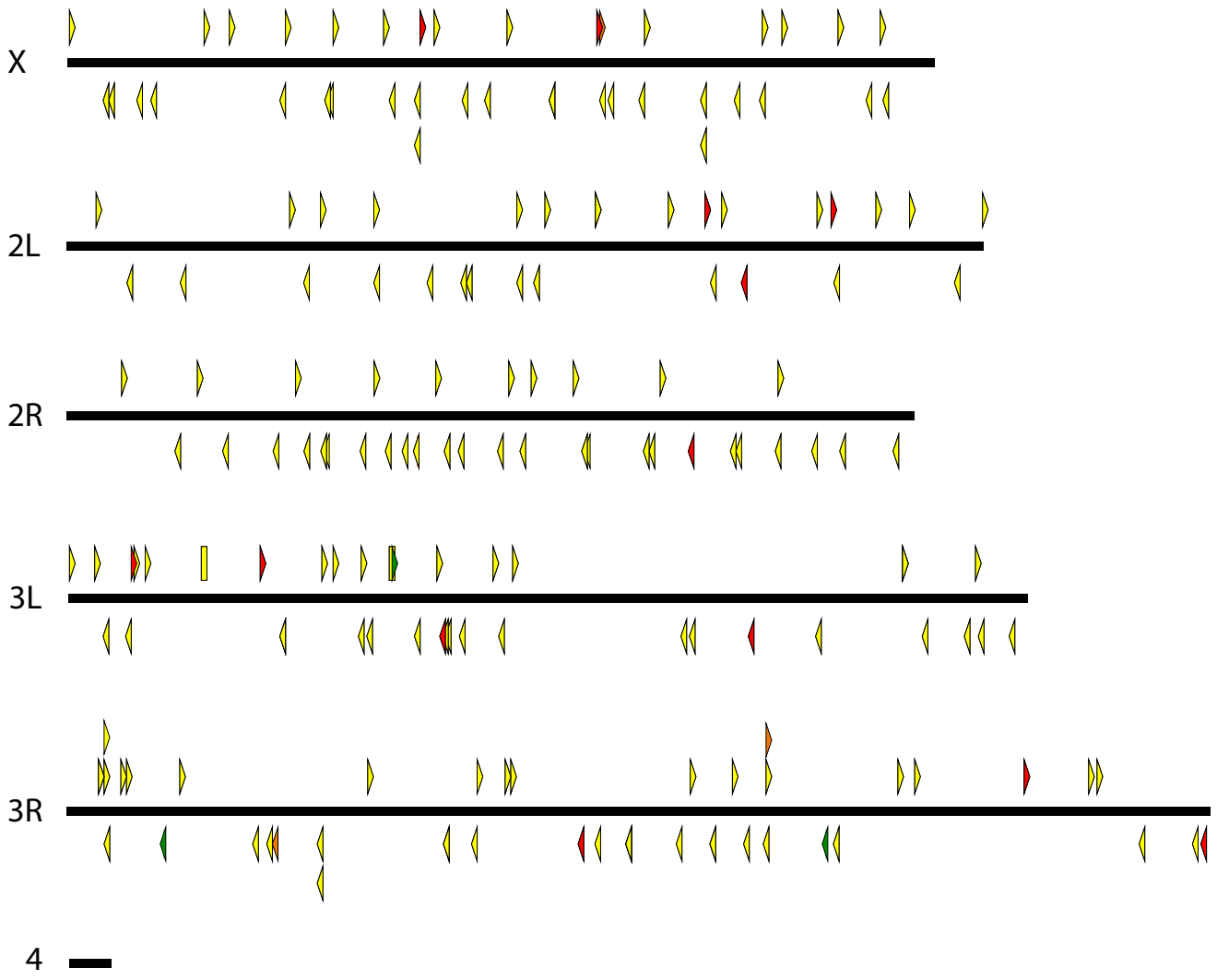

Figure 1. Genomic insertion sites of *pBac* transposable elements in *D. simulans*. Each triangle represents a unique *pBac* element insertion. Some strains carry multiple insertion events. Some insertion sites are present in multiple strains at least one of which contains multiple insertions. These strains were maintained to maximize the diversity of insertion sites in the collection. *pBac* insertions oriented forward are indicated above each chromosome and point to the right and reverse insertions are indicated below each chromosome and point to the left. Rectangles represent inserted elements whose orientation could not be determined. Yellow, green and red indicated elements carrying *3XP3*::*EYFP*, *3XP3*::*EGFP*, and *3XP3*::*DsRed*, respectively.

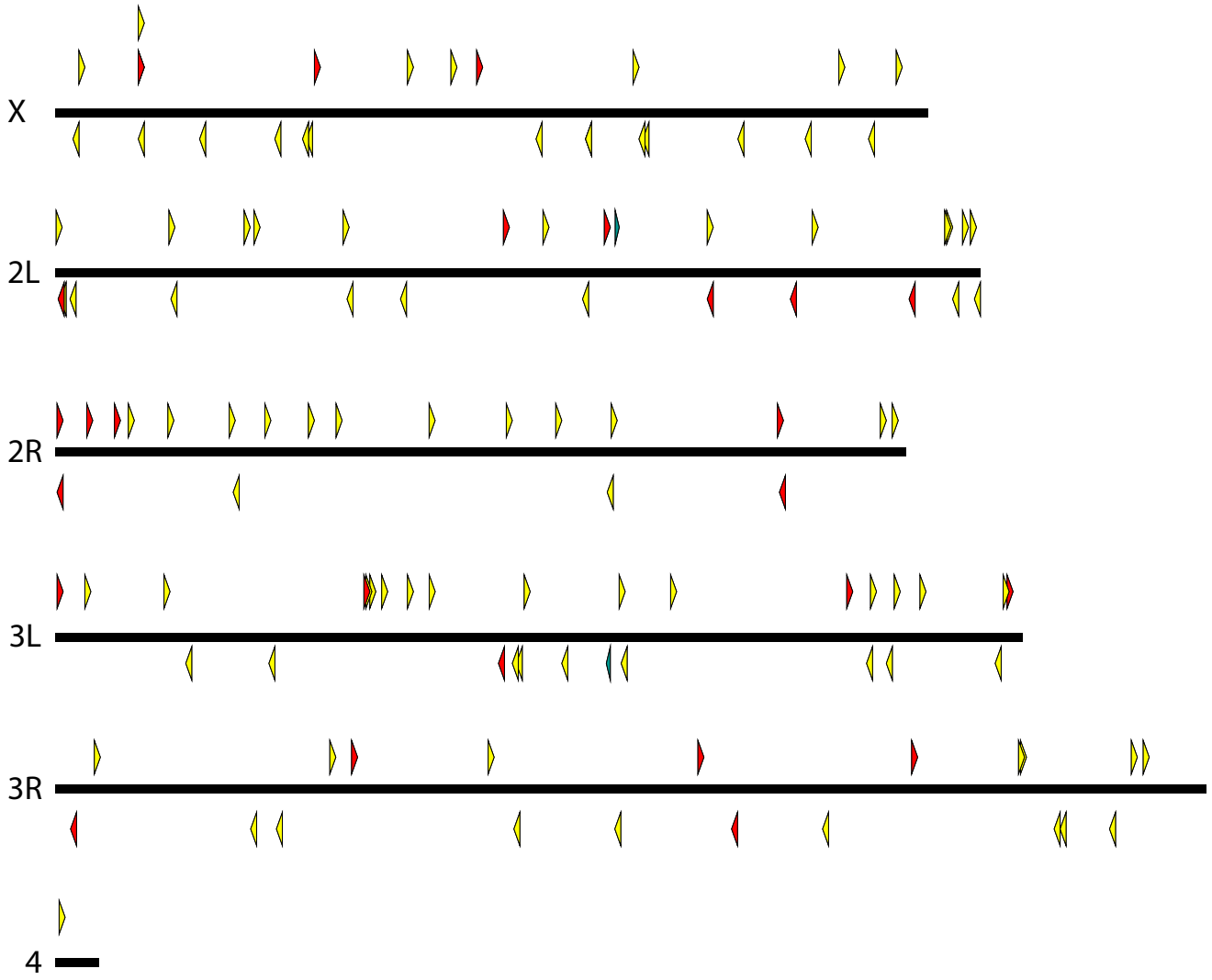

Figure 2. Genomic insertion sites of *pBac* transposable elements in *D. mauritiana*. Each triangle represents a unique *pBac* element insertion. Some strains carry multiple insertion events. Some insertion sites are present in multiple strains at least one of which contains multiple insertions. These strains were maintained to maximize the diversity of insertion sites in the collection. *pBac* insertions oriented forward are indicated above each chromosome and point to the right and reverse insertions are indicated below each chromosome and point to the left. Yellow, green and red indicated elements carrying *3XP3*::*EYFP*, *3XP3*::*EGFP*, and *3XP3*::*DsRed*, respectively.

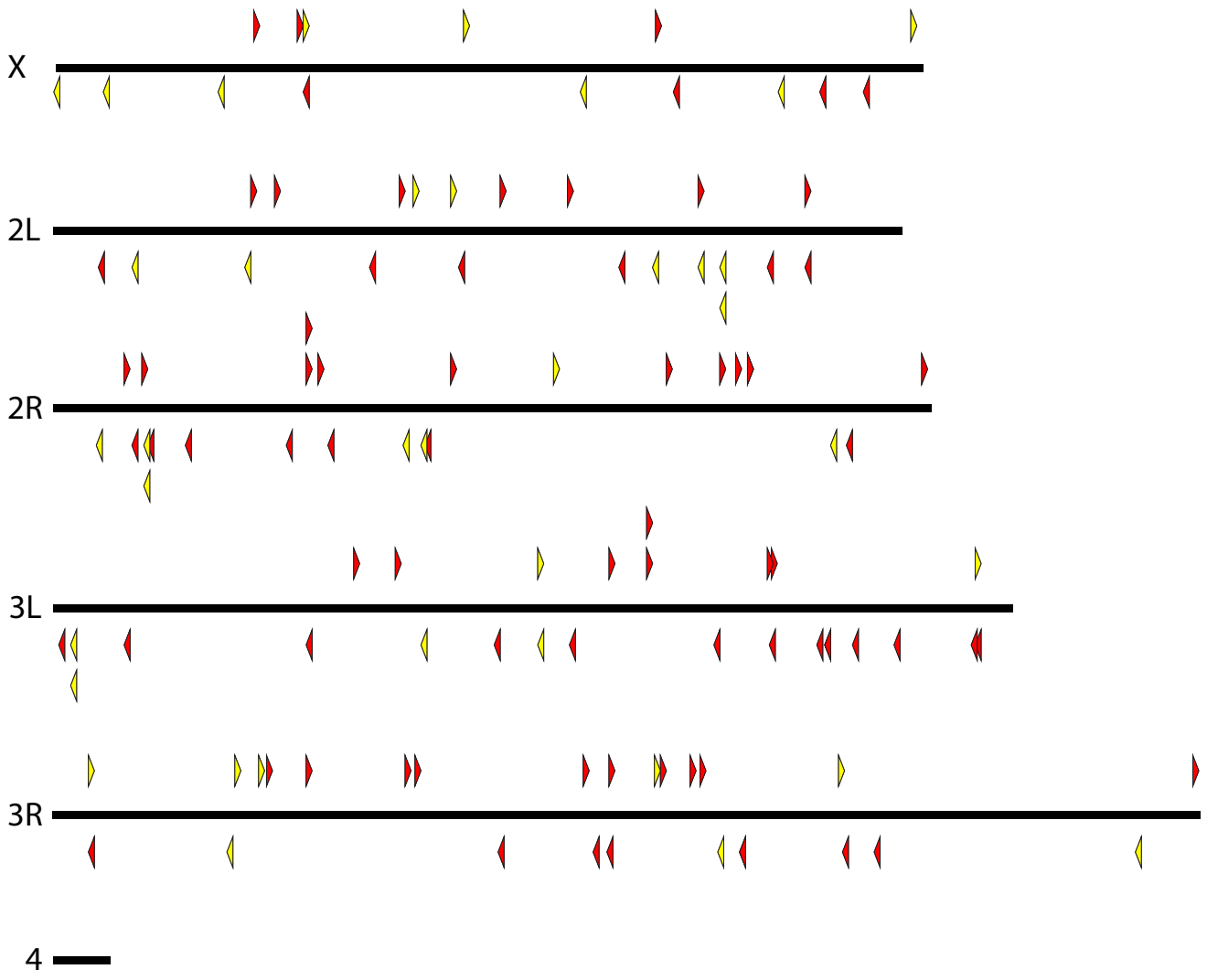

Figure 3. Genomic insertion sites of *pBac* transposable elements in *D. yakuba*. Each triangle represents a unique *pBac* element insertion. Some strains carry multiple insertion events. Some insertion sites are present in multiple strains at least one of which contains multiple insertions. These strains were maintained to maximize the diversity of insertion sites in the collection. *pBac* insertions oriented forward are indicated above each chromosome and point to the right and reverse insertions are indicated below each chromosome and point to the left. Yellow, green and red indicated elements carrying *3XP3*::*EYFP*, *3XP3*::*EGFP*, and *3XP3*::*DsRed*, respectively.

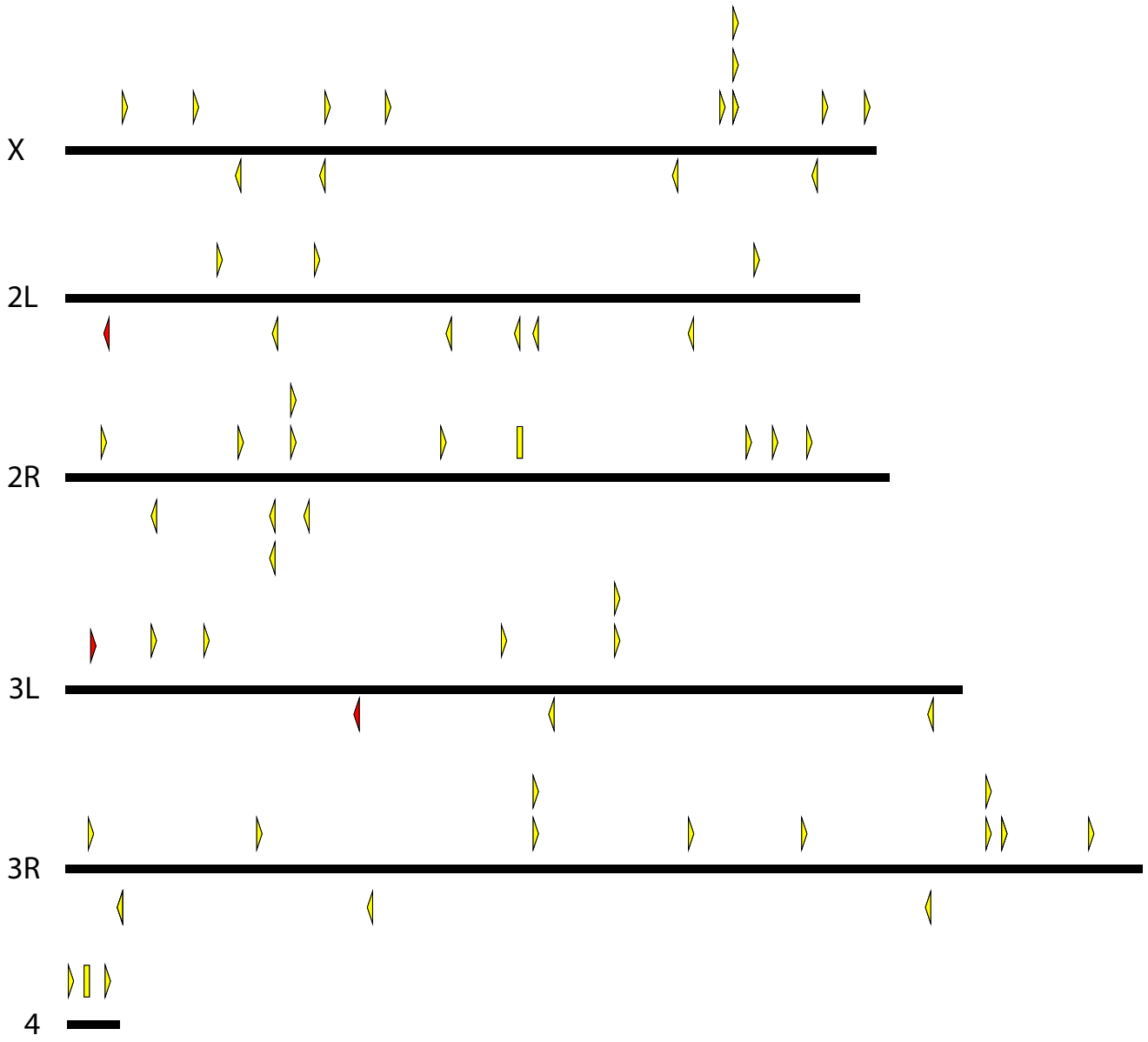

Figure 4. Genomic insertion sites of *pBac* transposable elements in *D. santomea*. Each triangle represents a unique *pBac* element insertion. Some strains carry multiple insertion events. Some insertion sites are present in multiple strains at least one of which contains multiple insertions. These strains were maintained to maximize the diversity of insertion sites in the collection. *pBac* insertions oriented forward are indicated above each chromosome and point to the right and reverse insertions are indicated below each chromosome and point to the left. Rectangles represent inserted elements whose orientation could not be determined. Yellow, green and red indicated elements carrying *3XP3*::*EYFP*, *3XP3*::*EGFP*, and *3XP3*::*DsRed*, respectively.

Figure 5. Genomic insertion sites of *pBac* transposable elements in *D. virilis*. Each triangle represents a unique *pBac* element insertion. Some strains carry multiple insertion events. *pBac* insertions oriented forward are indicated above each chromosome and point to the right and reverse insertions are indicated below each chromosome and point to the left. Yellow and orange indicated elements carrying *3XP3*::*EYFP* and w^+, respectively.

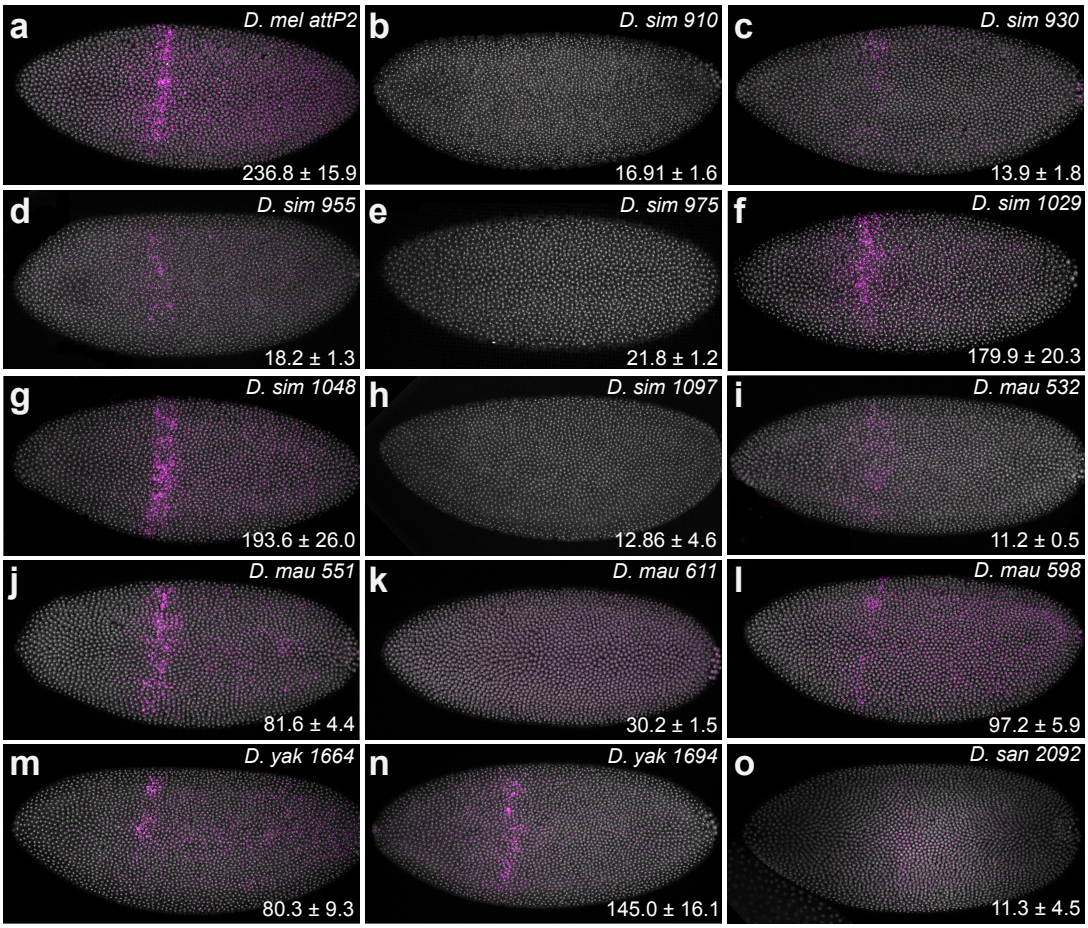

Figure 6. Variation in transgene expression supported by different *attP* landing sites in four species. An *eveS2* transgene driving expression in the *even-skipped stripe 2* domain of early embryos was inserted into multiple *attP* sites of each of four species: *D. simulans*, *D. mauritiana*, *D. yakuba*, and *D. santomea*. *eveS2* expression is shown in purple and DNA was counterstained with DAPI and shown in white. Expression levels in the stripe 2 domain were quantified in ten embryos of each strain and the mean ± standard deviation are reported in the bottom right corner of each panel in arbitrary units of fluoresence intensity. (**a**) As a control, we stained a line containing the same plasmid inserted into the *attP2* site of *D. melanogaster*. (**b-n**) Seven *attP* strains of *D. simulans* (**b-h**), four *attP* strains of *D. mauritiana* (**i-l**), and two *attP* strains of *D. yakuba* (**m**, **n**) support different levels of *eveS2* expression. (**o**) None of the four *D. santomea attP* strains we tested supported high levels of spatio-temporally correct *eveS2* expression. The strain displaying the strongest expression (*2092*) is shown in this here.

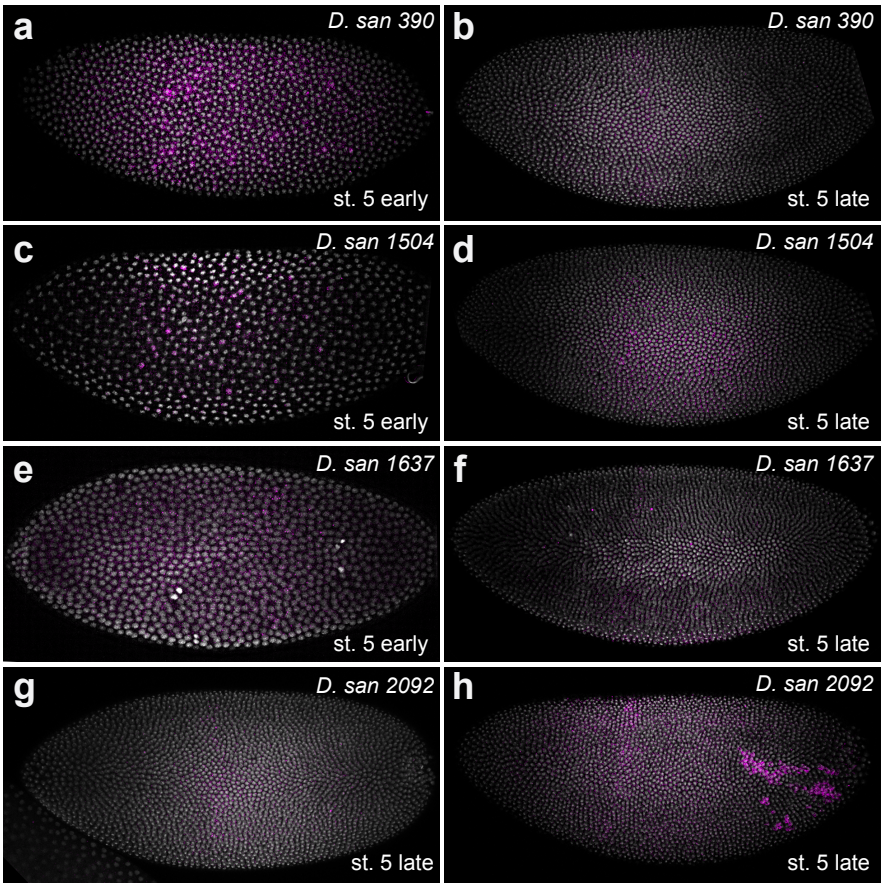

Figure 7. Four *D. santomea attP* landing sites do not support spatio-temporally correct *eveS2* transgene expression. (**a**-**g**) At early stage 5 embryonic stages, the lines displayed variable levels of diffuse expression, as is often observed with *eveS2* transgenes (**a**, **c**, **e**). However, at late stage5, none of the lines drove strong expression in the stripe 2 region (**b**, **d**, **f**, **g**). (**h**) Strain 2092 sometimes displayed strong ectopic expression outside of the stripe 2 domain.

Table 1. Number of *attP* strains of each of five species that did not or did allow integration of *attB* plasmids. Details are available in Supplementary File: Strains and Integration Efficiencies.xlsx.

Species	Number of strains with zero integrants	Number of strains with at least one integrant
D. mauritiana	14	21
D. simulans	13	29
D. santomea	1	8
D. yakuba	1	19
D. virilis	9	0